

Photochemical Reactions of Rhodium(III) Diimine Complexes in Solid Glycerol Matrixes. Thermal Activation of a Triplet 3dd Level from a Triplet $^3\pi\pi^*$ Manifold

J. A. Brozik and G. A. Crosby*

Department of Chemistry, Washington State University, Pullman, Washington 99164-4630

Received: August 20, 1997; In Final Form: October 17, 1997[⊗]

At temperatures below 150 K in rigid glycerol glasses, $[\text{Rh}(\text{III})(\text{s-NN})_3](\text{PF}_6)_3$ complexes display a $^3\pi\pi^*$ phosphorescence characteristic of the s-NN ligand [s-NN = 1,10-phenanthroline (phen), 4-Mephen, 4,7-Me₂-phen, and 3,4,7,8-Me₄phen]. Above 150 K but below the melting point of glycerol, a temperature-dependent first-order reaction occurs. The temperature dependences of these photochemical reactions conform to the Arrhenius equation with an activation energy range of 2500–3800 cm⁻¹. These results are interpreted in terms of the thermal redistribution of energy from the unreactive $^3\pi\pi^*$ excited term to a close-lying chemically active 3dd level. The relationship of the Arrhenius activation energies to the electronic structures and the spectra of the parent complexes is discussed. At 77 K all the photoproducts emit $^3\pi\pi^* \rightarrow \text{gs}$ phosphorescence. The spectral characteristics of the photogenerated species indicate that a single product has been produced in every case. Moreover, the energy of the phosphorescence of each photoproduct and its decay time at 77 K indicate that the newly generated species contains a monodentate s-NN ligand. We conjecture that one octahedral site on the metal is occupied by a glyceroxide moiety that is bonded directly to the rhodium ion through the oxygen atom.

Introduction

Luminescent (nd)⁶ transition metal complexes have received much attention from both spectroscopists and photochemists. A principal reason is that such complexes can be engineered to possess a variety of photochemical and photophysical properties through the judicious choice of the metal atom and coordinated ligands. Because the effects of spin-orbit coupling are significant in open-shell transition-metal complexes, the lowest excited triplet manifold usually dominates the photophysical properties of (nd)⁶ systems at low temperatures, but it is also clear that these lowest excited states are often significantly perturbed by close-lying upper excited states. In addition to providing static perturbations, at higher temperatures thermally accessible upper excited states are often responsible for changes in observable photophysical properties through opening additional deactivation channels leading to waxing or waning of luminescence intensity with increasing temperature. Thermally accessible excited states can also be responsible for competing photochemical reactions.

At higher temperatures the well-known ³MLCT emission of $[\text{Ru}(\text{bpy})_3]^{2+}$ is quenched by thermal population of a nonemissive 3dd term.¹ It is also clear that this 3dd term is responsible for photoinduced ligand loss in fluid solutions.^{2–7} A good example of a (nd)⁶ complex that exhibits luminescence properties complicated by the near coincidence of two excited states is $[\text{Rh}(3,3'\text{-Me}_2\text{bpy})_3](\text{ClO}_4)_3$, which displays bands that appear to arise from both $^3dd \rightarrow \text{gs}$ and $^3\pi\pi^* \rightarrow \text{gs}$ transitions. The bands display independent lifetimes in 77 K glasses but, as the temperature is raised above 231 K in a fluid acetonitrile solution, these systems appear to equilibrate and emit with a common lifetime.⁸ For $[\text{Rh}(\text{phen})_2(\text{NH}_3)_2]^{3+}$ it has also been reported that the phosphorescence is $^3\pi\pi^* \rightarrow \text{gs}$ in nature at 77 K in 1:1

ethylene glycol/water glasses, but as the temperature rises from 77 to 186 K a $^3dd \rightarrow \text{gs}$ luminescence grows in.⁹

Although the observed luminescences from the complexes $[\text{Rh}(\text{phen})_3]^{3+}$ and $[\text{Rh}(\text{bpy})_3]^{3+}$ are clearly $^3\pi\pi^* \rightarrow \text{gs}$ in nature, the 10² shortening of the lifetimes compared with those of the free ligands can be accounted for by perturbations from upper states lying near the lowest $^3\pi\pi^*$ manifold. Specifically, it has been shown through calculation that the lowest $^3\pi\pi^*$ level is perturbed by higher lying 3dd and $^3d\pi^*$ terms in $[\text{Rh}(\text{phen})_3]^{3+}$ and $[\text{Rh}(\text{bpy})_3]^{3+}$ and that these interactions are responsible for the reduced radiative lifetimes.^{10,11}

Recently, photochemical reactions of $[\text{Rh}(\text{phen})_3]^{3+}$ and $[\text{Rh}(\text{bpy})_3]^{3+}$ in solid glycerol glasses at temperatures above 150 K have been reported and the activation energies for this process have been measured. These reactions have been attributed to the thermal redistribution of energy from a chemically inert $^3\pi\pi^*$ level to a higher-lying 3dd manifold that immediately leads to a photochemical product.¹² The purpose of the present contribution is to quantify further the effect of tuning the lowest excited $^3\pi\pi^*$ level, through methyl substitution of the phen ligand, on the measured activation energy and to discuss the nature of the photoproduct.

Experimental Section

Syntheses. The α, α' -diimine ligands (s-NN = phen, 4-Mephen, 4,7-Me₂phen, 3,4,7,8-Me₄phen) were purchased from Aldrich and sublimed prior to use. $\text{RhCl}_3 \cdot \text{hydrate}$ (Aldrich) and ethanol (Mid-West Grain Products Co.) were used as received.

$[\text{Rh}(\text{s-NN})_3](\text{PF}_6)_3$ was prepared anaerobically from $\text{RhCl}_3 \cdot \text{hydrate}$ (1 mmol) and a slight excess of the diimine ligand (3.3 mmol) in a reaction vessel attached to a vacuum line. The solid reactants were degassed by maintaining them at a pressure below 1 mTorr for 12 h. An aqueous ethanol solution (2:1 ethanol/water) was rigorously degassed by three consecutive freeze–

[⊗] Abstract published in *Advance ACS Abstracts*, December 1, 1997.

pump-thaw cycles and condensed on the reactant mixture. Under gentle heating the slurry was stirred, and after ~ 2 h a clear light orange solution appeared. This solution containing the crude product was concentrated to ~ 15 mL on a hot plate by careful evaporation of the solvent. Precipitation was initiated by dropwise addition of the concentrate into acetone at 0°C . The precipitate was white with a tinge of pink. To effect purification a cation exchange column (12 in. \times 1 in. diameter; CM-Sephadex-C25) equipped with a Pharmacia UV detector and a stripchart recorder was employed. The eluant was water followed by solutions of NaCl stepped from 0.1 to 0.5 N (*vide infra*). The first colorless band came off with the water mobile phase. A second small yellow band was closely followed by a very small red band; both were eluted with 0.1 N NaCl. The largest band, containing colorless product, came off with the 0.3 N step. The final dark band was washed off the column with 0.5 N NaCl. Hexafluorophosphate salts of the complexes were produced through metathesis of the chlorides with a concentrated, filtered, neutralized solution of NaPF_6 . All complexes were obtained as white powders with yields between 84 and 93%.

Sample Preparation. All emission and lifetime measurements were performed on 10^{-4} M samples contained in glycerol. Monoprotonated ligands were prepared from a 1:1 mixture of ligand and HCl. For spectroscopic measurements samples of photoproducts were generated through exhaustive photolysis of 10^{-4} M $[\text{Rh}(\text{s-NN})_3(\text{PF}_6)_3]$ in glycerol glasses at 200 K. [The glycerol was vigorously degassed prior to use and samples were kept free of O_2 .] Measurements of photochemical reaction rates were conducted on 5×10^{-6} M solutions in rigorously degassed glycerol kept O_2 free under a stream of N_2 gas. Photochemical reaction rate measurements were always conducted on fresh samples.

Steady-State Emission. Steady-state emission spectra were obtained from samples mounted on small wire loops (2 mm diameter) suspended directly in liquid N_2 inside a quartz optical dewar. The excitation source was a LiCONIX 3305N HeCd laser that produced a 4 mW 325 nm line. The laser beam was passed through an aqueous solution of CuSO_4 followed by a Melles Griot UG-11 UV band-pass filter and aimed directly onto the sample. Emitted light was monitored at 90° to the excitation beam, filtered through an aqueous 33 M KNO_2 solution, dispersed by an Instruments SA HR-640 monochromator, and detected by a thermoelectrically cooled Hamamatsu R943-02 photomultiplier. The detector signal was passed through a wide-band preamplifier and fed to a Stanford Research Systems SR400 photon counter. Data were transferred to an IBM 386 PC for further manipulation. All spectra were corrected against a NBS spectral irradiance standard.

Lifetimes. For decay-time measurements at 77 K the sample preparation method and the detection system were as described above. The excitation light was chopped by either a rotating chopper or a mechanical shutter. An optical trigger synchronized the photon counter to the pulse train. The data were transferred to an IBM 386 PC for analysis. All data reduction was achieved by means of a curve-fitting program based on the simplex nonlinear search method.¹³

Measurement of Reaction Rates and Activation Energies. To measure photochemical rates, samples were contained in a thin film (~ 0.2 mm thick) on a wire loop. The film was thin enough to ensure uniform illumination. The loop was mounted directly on the specially designed thermostated fiber-optic sample rod depicted in Figure 1 and described below. With this setup any desired temperature between 77 and 300 K could

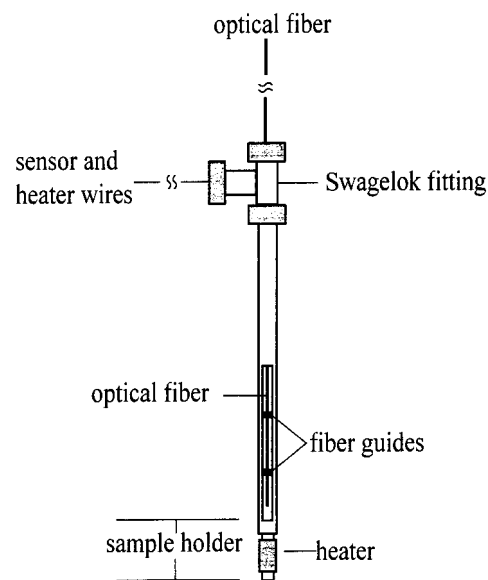


Figure 1. Fiber optic sample rod for measurement of temperature-dependent photochemical reaction rates.

be maintained. The main advantages of the sample rod are (a) illumination intensities are highly reproducible and (b) experiments can be conducted over a very long period of time (24 h with a 1 dm^3 storage dewar).

The sample rod body is a single piece of $1/2$ in. thin-walled stainless steel tubing containing two opposing 4 in. access windows starting $1/4$ in. from the bottom of the tube. To position the optical fiber in the center of the sample holder two identical optical fiber guides are mounted in the body (Figure 1). The sample holder is a single piece of copper with top diameter equal to the inside diameter of the sample rod body and a notch to provide access for heater wires. The bottom is $3/8$ in. in diameter and evenly wrapped with 40 ohms of nichrome heater wire protected by a thin evenly spread layer of five-minute epoxy. Offset from the center of the holder is a hole to accommodate a temperature sensor. The optical fiber, purchased from Fiberguide Industries, has a fused silica core of 0.6 mm diameter surrounded by a polyamide cladding. The fiber, protected by stainless steel needle stock, is 9 ft in length, and the ends are polished to an optical finish. The optical fiber, sensor wires, and heater wires lead through holes in Teflon stoppers that are held in place by a T-shaped Swagelok fitting (Figure 1).

The optical arrangement is depicted in Figure 2. A single fused silica optical fiber served for both excitation and detection. A front-surfaced aluminum mirror with a small hole (~ 1 mm diameter) drilled at 45° through its center allowed the 325 nm laser line (isolated as described above) to pass directly into the optical fiber. Emitted light emanating from the fiber was redirected 90° into the monochromator by the mirror. Although the end of the fiber closest to the mirror was never moved throughout the course of the experiments, the end closest to the sample was positioned flush against each freshly prepared glassy sample.

Samples were irradiated inside a 1 dm^3 liquid N_2 storage dewar in which the sample and rod were isolated from the liquid N_2 by a test tube. Temperature was controlled by the nichrome heater and a temperature controller (Lakeshore Crytronics TGC-100). The temperature was determined by monitoring the voltage drop across a cryodiode (CryoCal, Inc.), which was calibrated against fiducial temperatures of organic slushes. Excellent reproducibility was achieved.

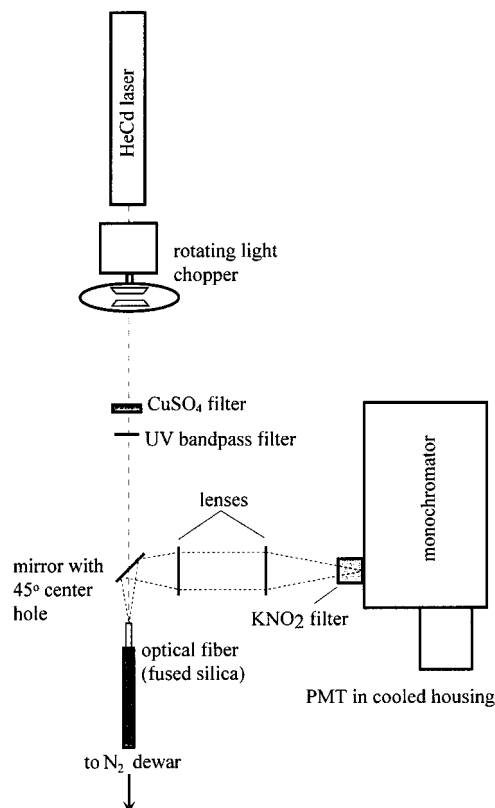


Figure 2. Optical arrangement for measurement of temperature-dependent photochemical reaction rates.

Although their spectra overlapped, the disparate lifetimes of the parent complexes and of their corresponding photoproducts permitted measurement of the photochemical reaction rates by simply monitoring the slow disappearance of the characteristic ${}^3\pi\pi^*$ emission of the parent. This was accomplished by chopping the excitation source at 12.5 Hz and recording the transient signal by means of the SR400 photon counter at a fixed delay time equal to 7.5 times the lifetime of the faster decaying photoproduct. Time-resolved emission spectra were taken at these settings to confirm that complete temporal separation had been achieved. Since the photoreaction rates were 10^2 – 10^3 slower than the chopping rate, depending on the temperature, chopping the excitation source had a negligible effect on the reaction rates. Activation energies were determined by fitting the photochemical data to the Arrhenius equation

$$\ln k_{\text{obs}} = -(\Delta\epsilon/k)(1/T) + \ln A$$

where k_{obs} is the observed reaction rate constant, $\Delta\epsilon$ is the activation energy, and k is the Boltzmann constant (in $\text{cm}^{-1} \text{K}^{-1}$).

Results

Emission Spectra. Shown in Figure 3 are the 77 K luminescence spectra of the monoprotonated ligands, the $[\text{Rh}(\text{s-NN})_3](\text{PF}_6)_3$ complexes, and the corresponding photoproducts. The spectra of the title complexes are all well-defined, highly structured ${}^3\pi\pi^* \rightarrow \text{gs}$ phosphorescences¹⁴ similar to those of the free ligands in the same glass (not shown). The energies of the emission maxima of the parent complexes decrease in the order $[\text{Rh}(\text{phen})_3](\text{PF}_6)_3 > [\text{Rh}(4\text{-Mephen})_3](\text{PF}_6)_3 > [\text{Rh}(4,7\text{-Me}_2\text{phen})_3](\text{PF}_6)_3 > [\text{Rh}(3,4,7,8\text{-Me}_4\text{phen})_3](\text{PF}_6)_3$.

Steady-state emission measurements on the photoproducts reveal intense phosphorescences with band shapes remarkably

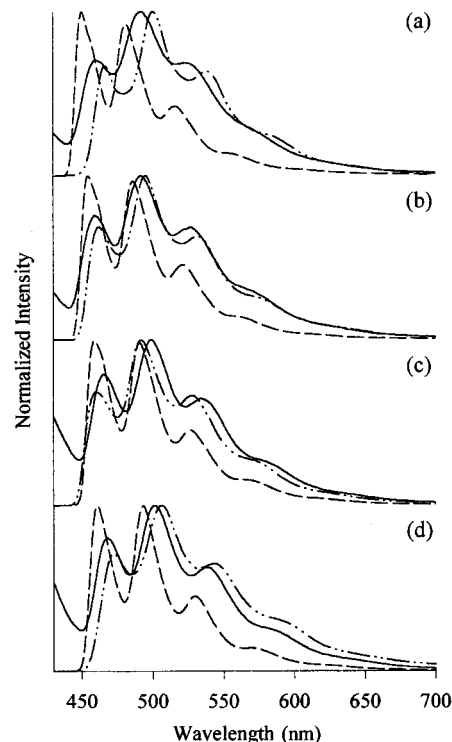


Figure 3. Steady-state emission spectra at 77 K of the monoprotonated ligands (—), $[\text{Rh}(\text{s-NN})_3](\text{PF}_6)_3$ (---), and the corresponding photoproducts (-·-·-) in glycerol glasses at 10^{-4} M: (a) phen, (b) 4-Mephen, (c) 4,7-Me₂phen, (d) 3,4,7,8-Me₄phen. Samples excited with a 325 nm HeCd laser line.

TABLE 1: Lifetimes of Monoprotonated Ligands, Parent Complexes, and Photoproducts at 77 K

	s-NN	s-NN:H ⁺ ^a	$[\text{Rh}(\text{s-NN})_3](\text{PF}_6)_3^a$	photoproduct ^a
phen		1.873	40.6×10^{-3}	2.09×10^{-3}
4-Mephen		2.018	44.5×10^{-3}	2.76×10^{-3}
4,7-Me ₂ phen		1.783	48.6×10^{-3}	2.42×10^{-3}
3,4,7,8-Me ₄ phen		1.938	44.5×10^{-3}	1.95×10^{-3}

^a All lifetimes in seconds.

similar to those of the corresponding monoprotonated ligands. Unlike the protonated ligands, however, the photoproducts emit no detectable fluorescence.

Lifetimes. The phosphorescence lifetimes of the monoprotonated ligands, parent tris complexes, and the photoproducts are listed in Table 1. Each decay curve was fit to a single exponential over five lives with excellent results. The phosphorescence decays of the monoprotonated ligands were on the order of 2 s, but when complexed to Rh(III) the corresponding ligand lifetimes decreased by 2 orders of magnitude. Lifetimes of the photoproducts were on the order of 2 ms, which corresponds to a shortening of about 3 orders of magnitude from those of the uncomplexed monoprotonated ligands.

Activation Energies. As previously reported for $[\text{Rh}(\text{phen})_3](\text{PF}_6)_3$ and $[\text{Rh}(\text{bpy})_3](\text{PF}_6)_3$,¹² the photochemical reaction rates for the title complexes are first order as determined by the rigorously exponential decrease of the phosphorescence intensity of each parent complex under constant illumination. We also confirmed that the reaction rates were independent of concentration but directly proportional to excitation intensity. As shown in Figure 4, the temperature dependence of the first-order reaction rates follows the Arrhenius equation yielding corresponding activation energies that range from 2500 to 3800 cm^{-1} (Table 2). Each point along a straight line was obtained from a fit to a single exponential over four natural lives. The reason

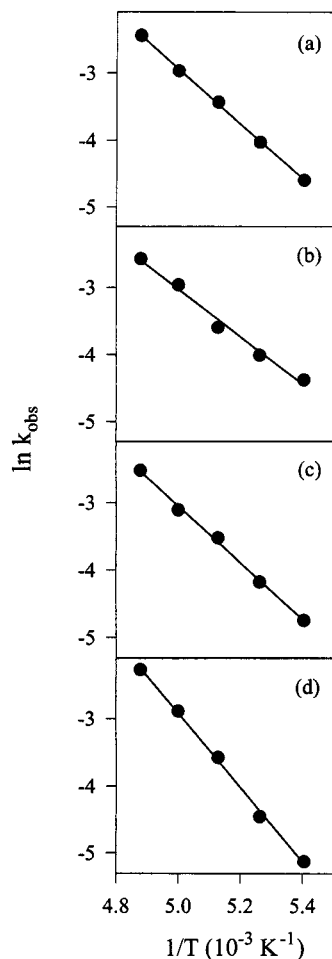


Figure 4. Arrhenius plots for the photochemical reaction of (a) [Rh(phen)₃](PF₆)₃, (b) [Rh(4-Mephen)₃](PF₆)₃, (c) [Rh(4,7-Me₂phen)₃](PF₆)₃, (d) [Rh(3,4,7,8-Me₄phen)₃](PF₆)₃.

TABLE 2: Summary of ³ππ* Energies and Arrhenius Activation Barriers

complex	first ³ ππ* → gs band max (cm ⁻¹)	activation energies (±50 cm ⁻¹)
[Rh(phen) ₃](PF ₆) ₃	22 200	2800
[Rh(4-Mephen) ₃](PF ₆) ₃	22 000	2500
[Rh(4,7-Me ₂ phen) ₃](PF ₆) ₃	21 800	2900
[Rh(3,4,7,8-Me ₄ phen) ₃](PF ₆) ₃	21 700	3800

for limiting the temperature range was 2-fold. At lower temperatures the reaction rates became too slow to measure precisely, and at higher temperatures the glass began to soften. The activation energies correlate roughly with the measured ³ππ* phosphorescence band maxima. Specifically, as the band maximum increases in energy the measured activation energy decreases (Table 2). The exception is the tris complex containing the asymmetric 4-Mephen ligand.

Chemical Properties of the [Rh(phen)₃](PF₆)₃ Photoproduct. The photoproduct of the prototypical complex, [Rh(phen)₃](PF₆)₃, was produced in bulk under anaerobic conditions in a specially designed low-temperature photoreactor.¹⁵ The photoproduct displayed ionic properties nearly identical with those of the parent complex. Specifically, under identical conditions the parent complex and its photoproduct were eluted from a CM-Sephadex-C25 cation exchange column with nearly the same volume of 0.3 N NaCl. Before isolation and subsequent drying, a steady-state emission spectrum of an aliquot of the purified product revealed no evidence for any starting material. Its spectrum was identical with the spectrum of the exhaustively

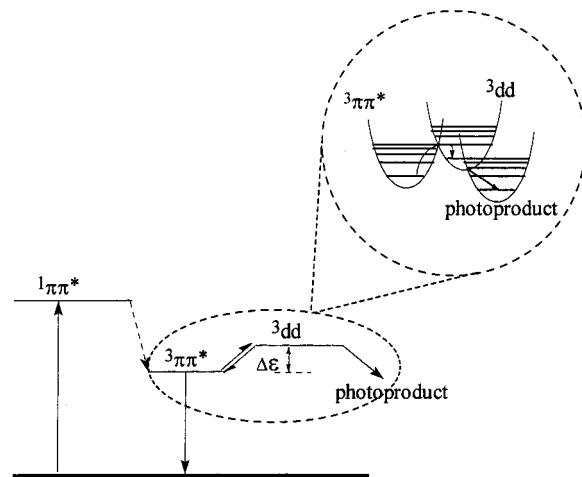


Figure 5. Proposed photophysical and photochemical pathway.

photolyzed sample depicted in Figure 3 (top---curve). The product was stable in solution. When isolated as a solid and dried in air, subsequent spectroscopic analysis revealed that nearly half of it had reverted back to the original [Rh(phen)₃](PF₆)₃ complex.

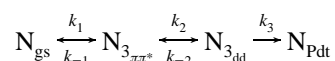
Discussion

Mechanistic Model. The observed photolysis curves correspond to first-order reactions. The simplest explanation is that the excited parent tris complex first reaches a ³ππ* level of the ligand system, from which it surmounts a barrier to the ground potential surface of the photoproduct, a process that involves no intervening electronic excited states of the parent molecule. The photochemical evidence suggests, however, that an isolated ³ππ* level does not lead to a photoreaction of this type. The internal standard is [Rh(5,6-Me₂phen)₃](PF₆)₃, which exhibits no photochemical reactivity under the conditions of these experiments.¹⁵ It does, however, display intense ³ππ* phosphorescence with nearly temperature-independent decay times from 4.2 K to the softening of the glycerol glass (~220 K).¹⁵ For the tris complexes that undergo a photochemical reaction there is ODMR evidence that both ³dπ* and ³dd configurations lie nearby and, through configurational mixing, are responsible for the ~10² shortening of the lives of the emissive ³ππ* manifolds in the complexes compared with the lifetimes of these same manifolds in the free ligands.¹⁰ We infer that one of these nearby configurations provides an intermediate state(s) in the photochemical pathway. We choose the ³dd for the following reasons: (a) the photoproduct of [Rh(phen)₃](PF₆)₃ possesses ionic properties that are nearly identical with those of the parent complex and (b) upon isolation and subsequent drying, a substantial amount of the product reverts back to the original starting material. The first observation suggests that no redox has occurred while the second provides evidence for substitutional photochemistry. Attributing the photochemical reactivity to a thermally accessible ³dπ* level appears to be insupportable because ³dπ* levels are known to promote redox chemistry, not substitutional photochemistry (a good example is [Ru(bpy)₃]²⁺). Conversely, ³dd levels are known to facilitate photosubstitution reactions. Examples include [Co(III)(NH₃)₆]³⁺, [RhX₂(NN)₂]⁺ (X = Cl⁻, I⁻),¹⁶ and [RhA₄X₂]⁺ (A = amine).¹⁷

A proposed scheme to account for the photochemistry by invoking the participation of a higher photoactive ³dd level is depicted in Figure 5. First, we assume that metal–ligand bonding and the ligand-field strengths of all the ligands are

similar, thus placing the nearby-lying 3dd level at essentially the same energy in each complex. According to this model the complex with the *highest* $^3\pi\pi^*$ energy should possess the *lowest* activation energy. This is in concert with the rough correlation between the $^3\pi\pi^*$ band maxima and the measured activation energies. This proposed mechanism also accounts for the photostability of $[\text{Rh}(\text{5,6-Me}_2\text{phen})_3](\text{PF}_6)_3$, which has a $^3\pi\pi^*$ level $\sim 2000\text{ cm}^{-1}$ lower than the rest of the tris complexes. Increasing the $^3\pi\pi^*$ - 3dd gap by this amount translates into a 10^6 slower photochemical rate, rendering this molecule essentially photoinert in the temperature range of the experiments. This proposed photochemical mechanism for these Rh(III) complexes accounts for the experimental results, is consistent with previous photochemical work, and is consistent with current knowledge of the properties of $^3\pi\pi^*$ and 3dd states.

Kinetic Analysis. To simplify the analysis we appeal to experimental information. Since no fluorescence was observed from these complexes, we assume the intersystem crossing rate to be very fast compared with the other postulated rates. Moreover, since the transient grow-in and decay of the $^3\pi\pi^*$ are much faster than the observed photochemical reaction rates, we assume the ground state and the $^3\pi\pi^*$ term to be in steady-state conditions during the entire course of the reaction. Hence, the scheme depicted in Figure 5 simplifies to



The assignment of the rate-determining step is based upon three experimental observations: (a) under no circumstances was any emission detected from a 3dd term, (b) the lifetimes from the related complexes $[\text{RhCl}_2(\text{s-NN})_2]^+$, known 3dd emitters, are on the order of $20\ \mu\text{s}$,¹⁴ and (c) when deuterated glycerol was substituted for glycerol there was no change in the measured activation energy or reaction rate. If k_3 were the rate-determining step, there would be a significant steady-state concentration of the 3dd manifold and emission from that set of levels should be observable, such as that readily detected from $[\text{RhCl}_2(\text{s-NN})_2]\text{Cl}$. No such emission was ever detected. In addition, the $^3dd \rightarrow \text{gs}$ emission lifetime is $\sim 20\ \mu\text{s}$ in $[\text{RhCl}_2(\text{s-NN})_2]\text{Cl}$. It is reasonable to believe k_3 would have to be at least competitive with this emission rate constant, but the measured reaction rates are all 10^5 – 10^8 slower than the lifetime expected for a 3dd manifold. Finally, if the photoreaction rate were limited by the rate of formation of the photoproduct from the 3dd manifold, one would expect a difference in the measured rate and activation energy when the reaction is carried out in deuterated glycerol. No such differences were observed. Consequently, we infer that the thermal redistribution of energy from $^3\pi\pi^*$ to 3dd is the rate-determining step. In other words, k_3 must be very rapid compared with k_2 and k_{-2} . This inequality has two major consequences. First, the $^3\pi\pi^*$ and 3dd levels are *not* in equilibrium; second, $k_{-2}N_{^3dd} \ll k_2N_{^3\pi\pi^*}$. The differential equations for the steady-state condition are

$$N_{^3\pi\pi^*}/N_{\text{gs}} = k_1/k_{-1} \text{ or } N_{^3\pi\pi^*}/N_{\text{gs}} = k_1/k_{-1} \quad (1)$$

$$dN_{^3\pi\pi^*}/dt = k_1N_{\text{gs}} + k_{-2}N_{^3dd} - (k_{-1} + k_2)N_{^3\pi\pi^*} \quad (2)$$

$$dN_{^3dd}/dt = k_2N_{^3\pi\pi^*} - (k_{-2} + k_3)N_{^3dd} \quad (3)$$

$$dN_{\text{Pdt}}/dt = k_3N_{^3dd} \quad (4)$$

Upon substitution and integration (see Appendix), the integrated rate laws for disappearance of the $^3\pi\pi^*$ level and the

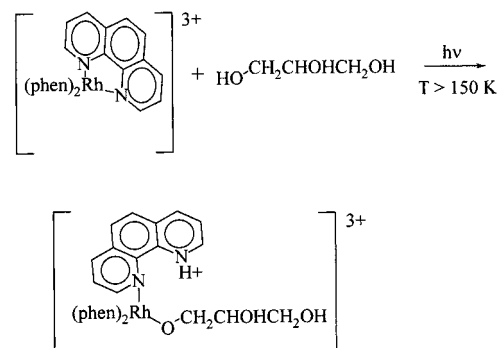


Figure 6. Proposed photochemical reaction.

grow-in of the photoproduct become

$$N_{^3\pi\pi^*}(t) = N_{^3\pi\pi^*}(0)e^{-k_2t} \quad (5)$$

$$N_{\text{Pdt}}(t) = N_{^3\pi\pi^*}(0)[1 - e^{-k_2t}] \quad (6)$$

This scheme implies that the rate of photoproduct production is proportional to the concentration of the 3dd manifold and that this concentration is related to the $^3\pi\pi^*$ concentration by the Arrhenius equation. Thus we write

$$k_2 = Ae^{-\Delta\epsilon/kT} \quad (7)$$

Expressions (5)–(7) account for the observed first-order rate law for the disappearance of a parent complex, the same first-order rate for the production of the corresponding photoproduct,¹⁵ the temperature dependence of each observed rate constant, and the dependence of the activation energy on the position of the $^3\pi\pi^*$ phosphorescence.

Although the *trends* of the activation energies and the $^3\pi\pi^*$ energies conform to the proposed model for the photochemical reaction, the *magnitudes* of the numbers differ considerably from the expected linear correlation. The discrepancies, which are far outside experimental error, could stem from the fact that the 3dd levels are not *exactly* the same energy for all complexes, or there is a different FC barrier to reaction in each compound. Either interpretation is reasonable, and both are probable.

Nature of the Photoproduct. The proposed photoreaction for the prototypical $[\text{Rh}(\text{phen})_3](\text{PF}_6)_3$ complex is depicted in Figure 6. The basis for postulating this simple reaction is as follows. Behavior of the photoproduct obtained from the bulk preparation indicated that no redox chemistry had occurred. This evidence strongly implies a photosubstitution reaction. Also, each photoproduct exhibits a luminescence spectrum almost identical with the phosphorescence observed from the corresponding monoprotonated uncomplexed ligand. Unlike the monoprotonated ligands, however, the photoproducts exhibit no fluorescence and have phosphorescence lifetimes shorter by 3 orders of magnitude than those of the protonated ligands. Since the lifetimes are so short and the fluorescence is quenched, we infer that the emitting chromophore must still be attached to the metal ion. From the close similarity of the emission spectra of the photoproducts and those of the corresponding protonated ligands (Figure 3), it is reasonable to conclude that one of the bidentate complexed ligands of the starting material becomes monodentate and protonated at the detached nitrogen atom as a consequence of irradiation. Moreover, the photoproducts and their parent complexes cannot be in equilibrium because the reactions can be driven to completion, and upon warming the

solutions to room temperature, the photoproducts do not revert back to the original starting complexes even after standing for 24 h.

The behavior of these rhodium complexes can be compared to that of $[\text{Ru}(\text{bpy})_2(3,3'\text{-Me}_2\text{bpy})]^{2+}$, which undergoes photo-substitution to form a monodentate intermediate upon irradiation in fluid solutions.¹⁸ The rate of conversion of this monodentate intermediate back to the original complex is substantially decreased by acid. Thus, it is reasonable to conclude that a proton is blocking the back reactions in these Rh(III) systems also. In order to account for the experimental data, we propose that a hydroxyl on glycerol attacks the excited Rh(III) ion, and the proton is transferred to the diimine N atom as the glyceroxide moiety bonds to the metal ion. Attachment of a glyceroxide to the metal appears reasonable because the reactions have been carried out in pure glycerol under rigorously anhydrous conditions where the only extrinsic entity for the complex to react with is a glycerol molecule. Attachment of the proton to the dangling N-atom of the bidentate ligand effectively blocks the back reaction.

Since the emission of each of the photoproducts is similar to that of the corresponding monoprotonated uncomplexed ligand and the transient decay is that expected for a spin-orbit perturbed spin-forbidden transition with primarily ligand orbital parentage, the photoproduct luminescence is assigned to a ${}^3\pi\pi^* \rightarrow \text{gs}$ phosphorescence from the monodentate s-phen:H⁺ ligand.

Appendix: Derivation of the Integrated Rate Laws

First solve for $N_{3\pi\pi^*}(t)$. We use eq 1 (steady-state condition) to eliminate N_{gs} in eq 2. The result is

$$dN_{3\pi\pi^*}/dt = k_{-2}N_{3\text{dd}} - k_2N_{3\pi\pi^*} \quad (\text{A1})$$

Since $k_{-2}N_{3\text{dd}} \ll k_2N_{3\pi\pi^*}$, eq A1 becomes

$$dN_{3\pi\pi^*}/dt = -k_2N_{3\pi\pi^*} \quad (\text{A2})$$

Integration of this equation yields eq 5

$$N_{3\pi\pi^*}(t) = N_{3\pi\pi^*}(0)e^{-k_2t} \quad (\text{5})$$

Accordingly, the disappearance of the characteristic ${}^3\pi\pi^*$ phosphorescence is first order. The second observable is the grow-in of the photoproduct, but first we solve for $N_{3\text{dd}}(t)$. Since $k_{-2}N_{3\text{dd}} \ll k_2N_{3\pi\pi^*}$, the expression in eq 3 reduces to

$$dN_{3\text{dd}}/dt = k_2N_{3\pi\pi^*} - k_3N_{3\text{dd}} \quad (\text{A3})$$

Substitution of $N_{3\pi\pi^*}(t)$ (eq 5) into eq A3 and rearranging the result yields

$$dN_{3\text{dd}}/dt + k_3N_{3\text{dd}} = k_2N_{3\pi\pi^*}(0)e^{-k_2t} \quad (\text{A4})$$

Multiplication of both sides of eq A4 by the integrating factor, $\mu = e^{k_3t}$, and rearrangement of the differential gives

$$d(e^{k_3t}N_{3\text{dd}}) = k_2N_{3\pi\pi^*}(0)e^{(k_3-k_2)t} dt \quad (\text{A5})$$

Integration of eq A5 from $t = 0$ to t produces

$$N_{3\text{dd}}(t) = [k_2N_{3\pi\pi^*}(0)/(k_3 - k_2)][e^{-k_2t} - e^{-k_3t}] \quad (\text{A6})$$

Since $k_3 \gg k_2$, eq A6 reduces to

$$N_{3\text{dd}}(t) = [k_2N_{3\pi\pi^*}(0)/k_3]e^{-k_2t} \quad (\text{A7})$$

To obtain the rate of grow-in of the photoproduct, one substitutes $N_{3\text{dd}}(t)$ (eq A7) into dN_{Pdt}/dt (eq 4) and integrates between 0 and t . The result is

$$N_{\text{Pdt}}(t) - N_{\text{Pdt}}(0) = (k_2/k_3)N_{3\pi\pi^*}(0)(e^{-k_2t} - 1) \quad (\text{A8})$$

Since at $t = 0$, $N_{\text{Pdt}} = 0$, eq A8 becomes

$$N_{\text{Pdt}}(t) = N_{3\pi\pi^*}(0)[1 - e^{-k_2t}]$$

Therefore, according to the model the photoproduct grows in with the same first-order rate constant as the decay of the ${}^3\pi\pi^*$ level of the parent complex. This equivalence has been experimentally confirmed for the photoreaction of $[\text{Rh}(\text{phen})_3]-(\text{PF}_6)_3$, and we infer that it holds for all the other systems.

Acknowledgment. Research was supported by a grant from the U.S. Department of Energy.

References and Notes

- (1) Allsopp, S. R.; Cox, A.; Kemp, T. J.; Reed, W. J.; Carassiti, V.; Traverso, O. *J. Chem. Soc., Faraday Trans. 1* **1978**, *74*, 1275.
- (2) Allsopp, S. R.; Cox, A.; Kemp, T. J.; Reed, W. J. *J. Chem. Soc., Faraday Trans. 1* **1979**, *75*, 353.
- (3) Lumpkin, R. S.; Kober, E. M.; Worl, L. A.; Murtaza, Z.; Meyer, T. J. *J. Phys. Chem.* **1990**, *94*, 239.
- (4) Van Houten, J.; Watts, R. J. *J. Am. Chem. Soc.* **1976**, *98*, 4853.
- (5) Van Houten, J.; Watts, R. J. *Inorg. Chem.* **1978**, *17*, 3381.
- (6) Wallace, W. M.; Hoggard, P. E. *Inorg. Chem.* **1980**, *19*, 2141.
- (7) Durham, B.; Caspar, J. V.; Nagle, J. K.; Meyer, T. J. *J. Am. Chem. Soc.* **1982**, *104*, 4803.
- (8) Nishizawa M.; Suzuki, T. M.; Sprouse, S.; Watts, R. J.; Ford, P. C. *Inorg. Chem.* **1984**, *23*, 1837.
- (9) Indelli, M. T.; Scandola, F. *Inorg. Chem.* **1990**, *29*, 3056.
- (10) Miki, H.; Shimada, M.; Azumi, T.; Brozik, J. A.; Crosby, G. A. *J. Phys. Chem.* **1993**, *97*, 11175.
- (11) Komada, Y.; Yamauchi, S.; Hirota, N. *J. Phys. Chem.* **1986**, *90*, 6425.
- (12) Brozik, J. A.; Crosby, G. A. *Chem. Phys. Lett.* **1996**, *255*, 445.
- (13) Demas, J. N.; Demas, S. N. *Interfacing and Scientific Computing on Personal Computers*; Allyn and Bacon: Needham Heights, MA, 1990.
- (14) Carstens, D. H. W.; Crosby, G. A. *J. Mol. Spectrosc.* **1970**, *34*, 113.
- (15) Brozik, J. A. Ph.D. Dissertation, Washington State University, 1996.
- (16) Gidney, P. M.; Gillard, R. D.; Heaton, B. T. *J. Chem. Soc., Dalton Trans.* **1972**, 2621.
- (17) Muir, M. M.; Zinner, L. B.; Paguaga, L. A.; Torres, L. M. *Inorg. Chem.* **1982**, *21*, 3448.
- (18) Tachiyashiki, S.; Ikezawa, H.; Mizumachi, K. *Inorg. Chem.* **1994**, *33*, 623.